JOURNAL OF GEOPHYSICAL RESEARCH, VOL. 102, NO. A8, PAGES 17,489–17,497, AUGUST 1, 1997

Evolution of the global aurora during positive IMF B_z and varying IMF B_y conditions

J. A. Cumnock [1] and J. R. Sharber
Southwest Research Institute, San Antonio, Texas

R. A. Heelis and M. R. Hairston
William B. Hanson Center for Space Sciences, University of Texas at Dallas, Richardson

J. D. Craven
Geophysical Institute and Physics Department, University of Alaska Fairbanks

Abstract. The DE 1 imaging instrumentation provides a full view of the entire auroral oval every 12 min for several hours during each orbit. We examined five examples of global evolution of the aurora that occurred during the northern hemisphere winter of 1981-1982 when the z component of the interplanetary magnetic field was positive and the y component was changing sign. Evolution of an expanded auroral emission region into a theta aurora appears to require a change in the sign of B_y during northward interplanetary magnetic field (IMF). Theta aurora are formed both from expanded duskside emission regions (B_y changes from positive to negative) and dawnside emission regions (B_y changes from negative to positive), however the dawnside-originating and duskside-originating evolutions are not mirror images. The persistence of a theta aurora after its formation suggests that there may be no clear relationship between the theta aurora pattern and the instantaneous configuration of the IMF.

1. Introduction

During intervals of northward interplanetary magnetic field (IMF), the auroral oval is contracted to higher latitudes and often exhibits broad emission regions in the dawn and dusk sectors that can spread poleward to very high latitudes. Where these regions form in local time is dependent on the sign of B_y: in the northern hemisphere an emission region forms on the duskside of the noon-midnight meridian when B_y is positive and an emission region forms on the dawnside when B_y is negative [*Hones et al.*, 1989]. When average B_y is approximately zero, emission regions often form on both the dawn and dusk sides of the auroral oval forming a "teardrop-shaped" region near the pole which is void of auroral emissions [*Murphree et al.*, 1982]; this pattern is sometimes referred to as the "horse-collar aurora" [*Hones et al.*, 1989]. It is believed that this expansion of the auroral oval results from a poleward expansion of a region of closed field lines which map to the plasma sheet boundary layer of the magnetosphere [*Meng*, 1981]. This view is supported by the studies of *Birn et al.* [1991] and *Elphinstone et al.* [1991] using the *Tsyganenko* [1987] magnetic field model. Other recent studies confirm agreement between far-ultraviolet (FUV) signatures and particle precipitation patterns [*Sharber et al.*, 1992; *Lassen et al.*, 1988].

In addition, during magnetically quiet intervals large-scale Sun-aligned transpolar arcs can be observed to extend across the polar region from the local-noon sector to the midnight sector. These patterns tend to be associated with larger IMF B_z values, and greater IMF magnitude in general, than the horse-collar pattern [*Burch et al.*, 1992]. The motion and location of the transpolar arcs is often dependent on the sign of B_y, with the transpolar arcs moving toward the duskside of the noon-midnight meridian in the northern hemisphere when B_y is positive [*Huang et al.*, 1989] and toward the dawnside when B_y is negative [*Frank et al.*, 1985; *Craven and Frank*, 1991]. Motion of the transpolar arc is seen to be in the opposite direction in the southern hemisphere [*Craven et al.*, 1991]. The auroral pattern made up of the transpolar arc and the oval has also been called "theta aurora" [*Frank et al.*, 1982]. Particle measurements on field lines above the transpolar arc of the theta aurora indicate that those field lines may originate in the plasma sheet boundary layer. This may occur as an isolated region surrounded by particles normally associated with the polar cap, indicating a bifurcated magnetotail [*Frank et al.*, 1982, 1986; *Bythrow*

[1]Now at Space Physics Research Laboratory, University of Michigan, Ann Arbor.

Paper number 97JA01182.
0148-0227/97/97JA-01182$09.00

et al., 1985], or as part of an extended region of auroral precipitation [*Eliasson et al.*, 1987], indicating a large dawn-dusk asymmetry in the plasma sheet or a significant "distortion" in the mapping along field lines between the ionosphere and the magnetotail [*Blomberg and Marklund*, 1993].

Ionospheric convection patterns observed during northward IMF consist of a variety of configurations including spatially dominant one-cell patterns and multiple-cell patterns. The number of cells appears to have a first-order dependence on the ratio of B_z to B_y, resulting in an increasing number of cells as the IMF becomes more strongly northward [*Potemra et al.*, 1984; *Reiff and Burch*, 1985; *Heelis et al.*, 1986; *Cumnock et al.*, 1995, and references therein]. Attempts have been made to reconcile instantaneous auroral-arc observations with theoretical models of convection [*Reiff et al.*, 1978; *Chiu et al.*, 1985; *Jankowska et al.*, 1990] and models of the

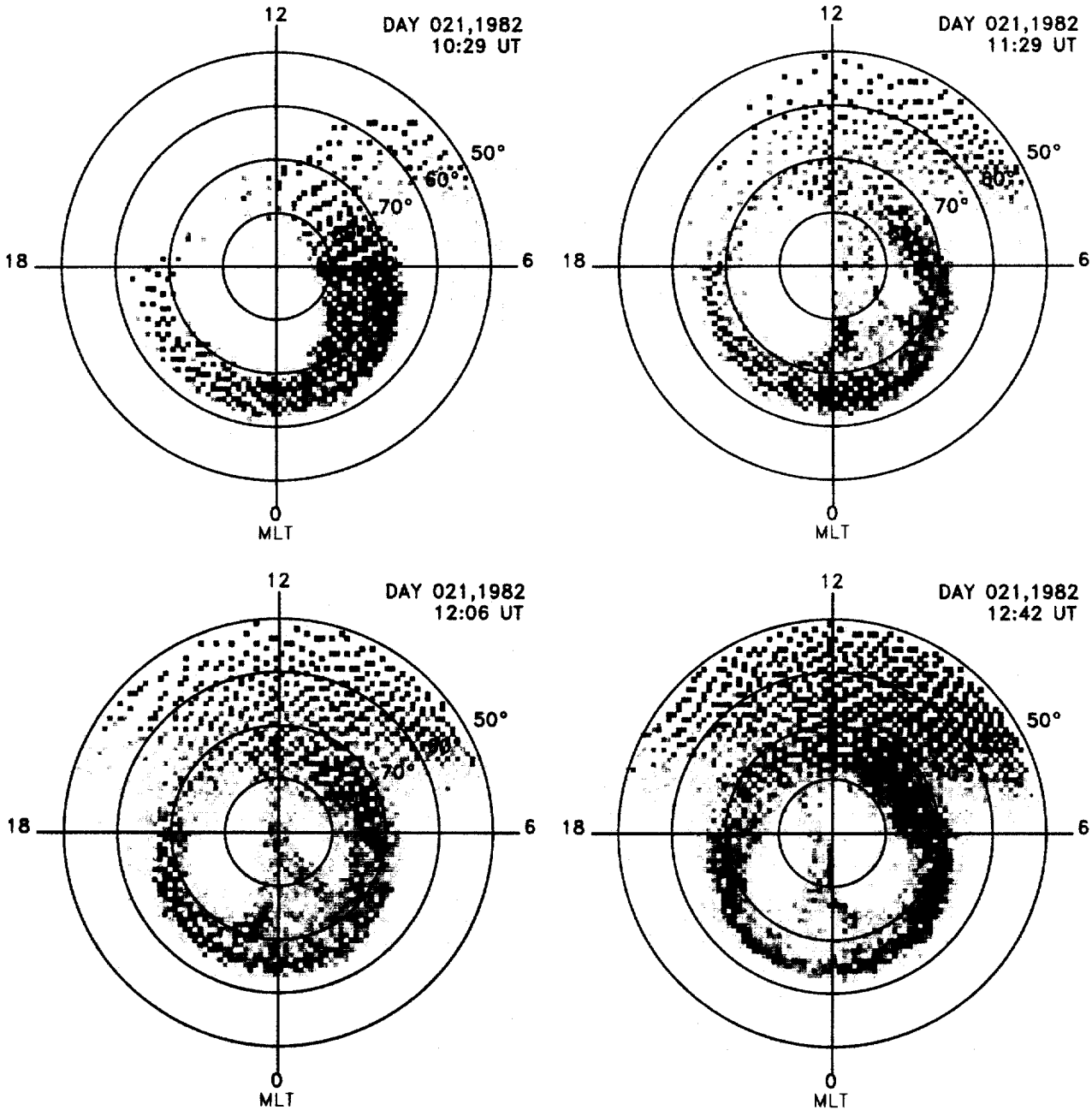

Plate 1. False-color images beginning at 1029 UT, 1129 UT, 1206 UT, and 1242 UT on day 21 of 1982. The images of northern hemisphere auroral luminosities (123 - 155 nm passband) taken by the DE 1 auroral imager are projected into a magnetic local time - corrected geomagnetic latitude coordinate system. The color bar extends from light orange to red to represent the lowest to highest intensities ($\sim$ 1 kR to $\sim$ 55 kR). Luminosities less than 1 kR are coded light yellow. Day and time, at the upper right in each image, denote the beginning of an image taken over a 12-min period.

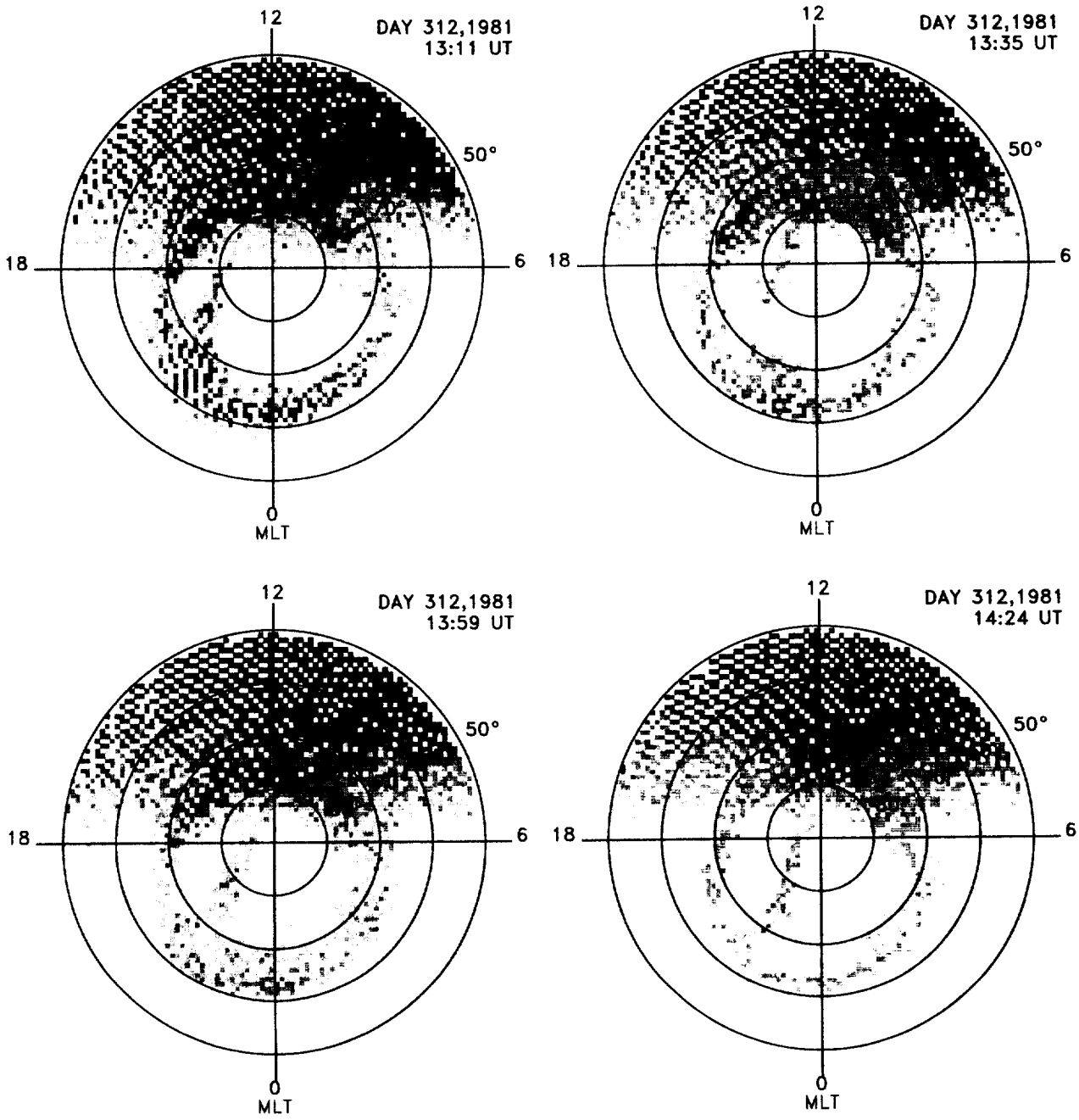

Plate 2. False-color images beginning at 1311 UT, 1335 UT, 1359 UT, and 1424 UT on day 312 of 1981; same format as Plate 1.

large-scale magnetospheric configuration [*Lundin et al.*, 1991; *Weiss et al.*, 1993, and references therein].

It has been reported that the "horse-collar aurora" sometimes evolves into the theta pattern [*Hones et al.*, 1989]. Here we examine several examples (and show two examples), from the Dynamics Explorer 1 satellite (DE 1), in which a series of images show this large-scale spatial evolution of the global auroral pattern during changing northward IMF. We reconcile large-scale changes in the global auroral pattern with the large-scale ionospheric plasma convection, consistent with observations of the influence of the IMF.

2. Observations

Auroral images are obtained from the DE 1 satellite, launched in August 1981, with an altitude of 3.65 R_E (Earth radius) at apogee, 570 km at perigee and a 90° orbital inclination. An initial latitude of 78.2°N at apogee permits views of the northern polar region. The DE 1 imaging instrumentation provides a full view of the entire auroral oval every 12 min for typically 3 hours in each orbit and permits imaging of the aurora in the sunlit atmosphere through the use of filters in several FUV wavelength bands. For example, with fil-

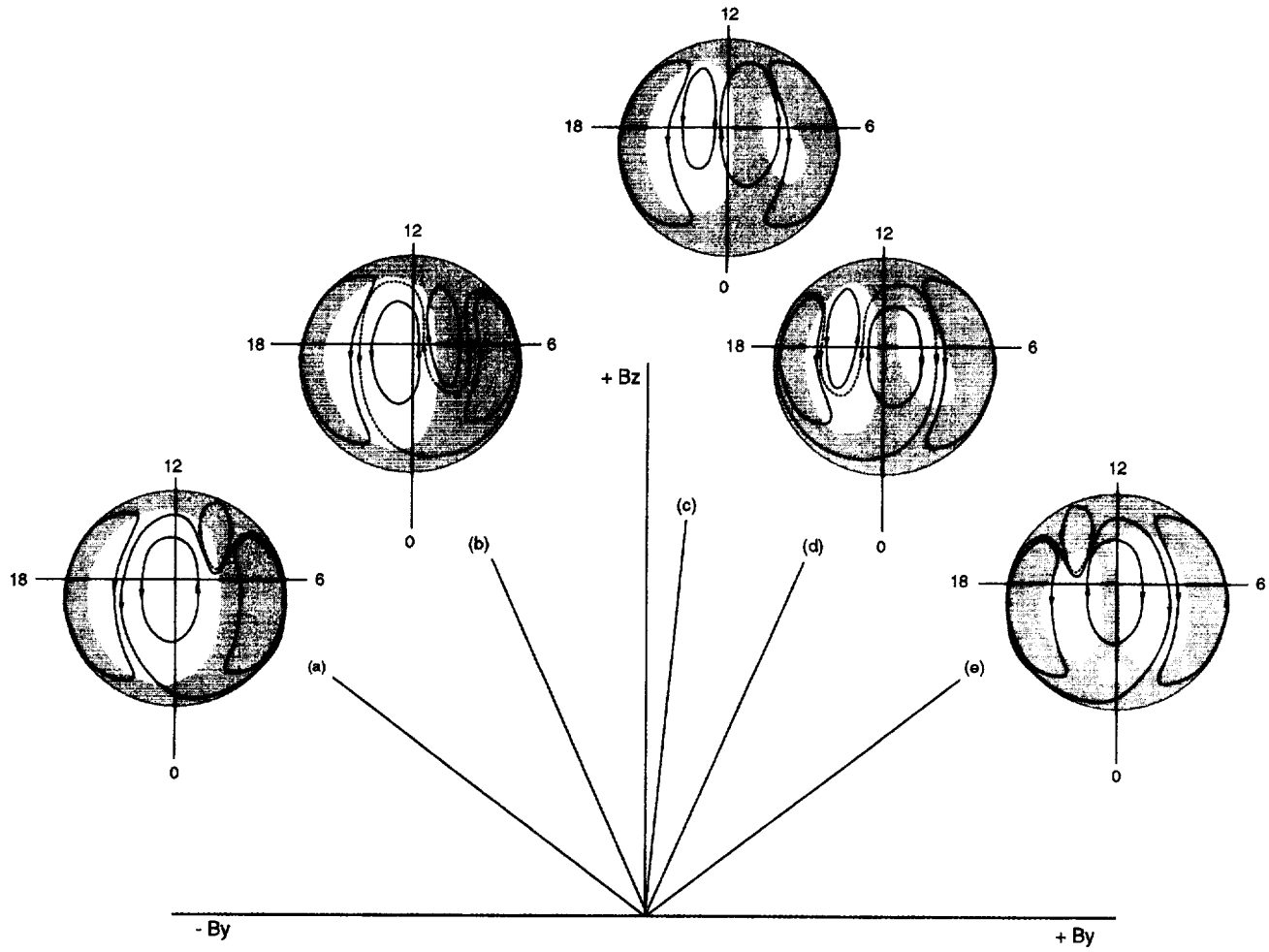

Plate 3. A sequence of schematic aurora and global ionospheric convection patterns which are consistent with observations of the aurora seen in Plate 1 and an evolution of the convection pattern. The polar schematics are organized by IMF orientation (in the B_y-B_z plane). The most significant changes in global configuration are shown as B_y changes from (a,b) negative on the left-hand side to (c-e) positive on the right-hand side. Auroral luminosities are illustrated in red; solid black lines denote lines of equipotential forming simple convection cells, and dotted black lines show another possible closure of the plasma flows indicated by equipotentials.

ter 2 (used in this study) at FUV wavelengths 123 to 155 nm, the principal emissions from the aurora along the oval and within the polar cap are from atomic oxygen (O I) at about 130.4 and 135.6 nm. For details see *Frank et al.* [1981] and *Frank and Craven* [1988]. For the satellite near apogee the spatial dimension of one pixel is about 120 km at auroral altitudes.

We examined 5 examples of global evolution of the aurora that occurred during the northern hemisphere winter of 1981-1982, but show only two of the examples which are representative of the large-scale features in all of the observations. In the first (Plate 1, day 21 of 1982) a theta aurora evolves from an expanded dawnside emission region and during the second (Plate 2, day 312 of 1981) the theta aurora originates on the duskside. What appears to be a single continuous arc (for example, Plate 1, 1242 UT and Plate 2, 1424 UT) may, because of image resolution, in fact be several isolated arc structures [see *Frank et al.*, 1986]. Also note that formation, disappearance and motion of arcs can occur within the 12-min period during which an image is formed, although the scan across the arc itself takes much less time, depending on geometry.

For a few of the auroral images examined here, Dynamics Explorer 2, the low-altitude companion satellite in the same orbital plane as DE 1, provides the horizontal plasma drift from low altitudes. Variations in the plasma drifts are used to estimate a reasonable large-scale global convection pattern.

ISEE 3 provides magnetic field measurements used to determine IMF orientation prior to and during the DE 1 imaging periods. Figure 1 shows ISEE 3 interplanetary magnetic field data B_x, B_y, and B_z (nanotesla) for the two examples illustrated in the study, day 21 of 1982 and day 312 of 1981. The times of the beginning of the northern high-latitude DE 1 images are indicated by the

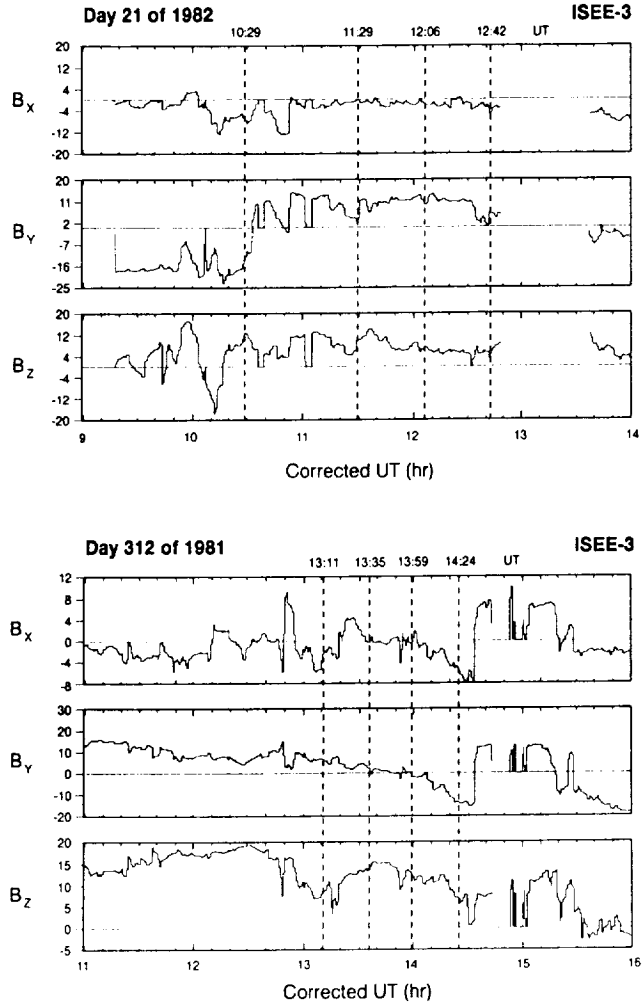

Figure 1. ISEE 3 interplanetary magnetic field data B_x, B_y, and B_z (nanotesla) for the two examples illustrated in the study, day 21 of 1982 and day 312 of 1981. The 1-min averages of the IMF are plotted in GSE coordinates as a function of corrected universal time (universal time plus the estimated time of propagation from ISEE 3 to the Earth's magnetopause of approximately 1 hour). At these times ISEE 3 was operating at the L1 point, $\sim 240\ R_E$ sunward of the Earth. The times at the beginning of the northern high-latitude DE 1 images are indicated by the dashed lines.

dashed lines. The 1-min averages of the IMF are plotted in GSE coordinates as a function of corrected universal time (universal time plus the estimated time of propagation from ISEE 3 to the Earth's magnetopause). During this time period, ISEE 3 was operating at the L1 point, $\sim 240\ R_E$ sunward of the earth, resulting in a time delay between an IMF measurement at ISEE 3 and that appropriate at the magnetopause of approximately 1 hour. Consequently, because of the location of ISEE 3, the IMF does not necessarily maintain the same orientation in its transit to the Earth. Hourly averages of the solar wind velocity are also available from this database.

False-color images of auroral luminosities are presented in Plate 1 and Plate 2, with the color bar extending from light orange to red to represent the lowest to highest intensities ($\sim$ 1 kR to $\sim$ 55 kR). Luminosities less than 1 kR are coded light yellow. These are not the actual satellite images, but a projection of the data onto a common coordinate system so the reader can more easily compare them. The images are plotted in magnetic local time (MLT) and corrected geomagnetic latitude (CGL) utilizing data and software provided by the National Space Science Data Center (NSSDC). Day and time, at the upper right in each image, denote the beginning of an image taken over a 12-min period.

Day 21, 1982 (0952-1408)

Plate 1 shows a sequence of four auroral images selected from the time interval 0952-1408 UT on Day 21 of 1982. The IMF for this time period is shown in the top three panels of Figure 1, plotted as a function of corrected UT. IMF B_z is northward throughout this time period while IMF B_y changes from negative to positive. The 15-min average of the IMF just prior to the image start time (denoted by the dashed line in Figure 1) is used in our analysis in order to characterize the IMF conditions applicable to the observed pattern. The solar wind velocity is greater than average (> 400 km/s).

During the image beginning at 1029 UT, B_z is positive and B_y is negative, with the magnitude of B_y slightly greater than the magnitude of B_z ($B_z/|B_y| \leq 1$). Note that the afternoon section of the auroral oval is not in the field of view of the satellite. The dawnside of the auroral oval has expanded poleward (as expected for negative B_y).

B_y then changes sign from negative to positive, and by approximately 1117 UT the poleward edge of the dawnside emission region had expanded poleward to within 2° of the noon-midnight meridian. At the time of the image beginning at 1129 UT, the magnitude of B_y is a little less than the magnitude of B_z ($B_z/B_y \geq 1$). The poleward edge of the dawnside emission region has moved farther duskward and is now located at the noon-midnight meridian. In addition to a large cleared region on the duskside, a small cleared region now exists in the dawnside emission region located at approximately 85° CGL near the dawn-dusk meridian.

IMF B_y continues to increase so that during the image beginning at 1206 UT the magnitude of B_y is much larger than the magnitude of B_z ($B_z/B_y \ll 1$). A theta aurora has fully formed, with the transpolar arc aligned along the noon-midnight meridian. The cleared region on the duskside is still spatially larger than the cleared region on the dawnside.

By 1242 UT B_y has decreased so that the magnitude of B_y is less than the magnitude of B_z ($B_z/B_y > 1$). The transpolar arc has moved to the duskside of the noon-midnight meridian and the duskside emission region has expanded weakly poleward so that the cleared region on the dawnside is now spatially larger than the

cleared region on the duskside. The transpolar arc appears to bifurcate in the nightside polar cap and to intersect the nightside oval in two places. IMF B_y changes sign from positive to negative after this image, and the transpolar arc begins to move back toward the dawnside (as expected with negative B_y).

We also examined the images for day 28 of 1982 where similar IMF conditions existed. While we do not present the images here, they essentially follow the same progression of an enhanced dawnside emission region evolving into a theta aurora with generally similar large-scale characteristics as those shown in Plate 1.

Day 312, 1981 (1234-1637 UT)

Plate 2 shows a sequence of four auroral images selected from the time interval 1234-1637 UT on day 312 of 1981, which is the time period of the first reported theta aurora [*Frank et al.*, 1982]. The IMF for this time period is shown in the bottom three panels of Figure 1. IMF B_z is northward and IMF B_y changes from positive to negative. The solar wind velocity is greater than average (> 400 km/s).

During the image beginning at 1311 UT, B_y and B_z are both positive with the magnitude of B_y a little less than the magnitude of B_z ($B_z/B_y \geq 1$). The duskside of the auroral oval has expanded poleward (as expected for positive B_y) with the poleward edge of the emission region located midway between the duskside equatorward edge of the auroral oval and the noon-midnight meridian.

By 1335 UT, B_y has decreased to near zero while B_z has increased, resulting in the magnitude of B_y being much less than B_z ($B_z/B_y \gg 1$). The poleward edge of the duskside emission region has moved to slightly higher latitudes, and some clearing of this emission region has occurred at approximately 85° CGL near the dawn-dusk meridian.

During the image beginning at 1359 UT, B_y has turned weakly negative so that the magnitude of B_y is much less than B_z ($B_z/|B_y| \gg 1$). The poleward edge of the transpolar arc has moved to slightly higher latitudes. A little more clearing of the emission region has occurred forming a more developed arc.

B_y continues to decrease until the magnitude of negative B_y is slightly less than B_z ($B_z/|B_y| \geq 1$). During the image beginning at 1424 UT a theta aurora has fully formed, with the transpolar arc located near the noon-midnight meridian. Movement of the transpolar arc is from dusk to dawn, as expected for negative B_y. The arc appears to intersect the nightside oval in two places (similar to Plate 1, 1242 UT). At about 1435 UT B_y changes sign from negative to positive and the transpolar arc moves back toward the duskside (as expected with positive B_y).

We also examined the images for days 329 and 363 of 1981 where similar IMF conditions existed. Although we do not present the images here, they essentially follow the same progression of an enhanced duskside emission region evolving into a theta aurora with generally similar large-scale characteristics as those shown in Plate 2.

3. Auroral Evolution and Large-Scale Plasma Convection

The evolution of the aurora and the motion of the sun-aligned arcs may be related in a self-consistent manner to the horizontal plasma convection in the ionosphere. The theta aurora is observed to evolve as the IMF becomes more strongly northward with a corresponding change in the sign of B_y. In the ionospheric plasma flows, a similar IMF rotation produces an increasing number of plasma convection cells (e.g., evolution from a dominant one-cell pattern to reverse convection at highest latitudes [*Potemra et al.*, 1984; *Reiff and Burch*, 1985; *Heelis et al.*, 1986; *Cumnock et al.*, 1995, and references therein]). Although DE 2 horizontal plasma flow data were not available associated with the DE 1 imaging sequences examined here, several passes were available for various theta aurora previously published by *Frank et al.* [1986], *Carlson et al.* [1988], and *Nielsen et al.* [1990]. These references show convection patterns coincident with theta auroras. The DE 2 data indicate that the Sun-aligned arcs are colocated with regions of upward flowing currents on the duskside of the polar region and weaker upward current sheets embedded in a downward current sheet on the dawnside of the polar region. The association of large-scale auroral arcs with upward flowing current was demonstrated by *Kamide and Akasofu* [1976] and *Burch and Heelis* [1979]. Upward flowing currents may be reconciled with gradients in the plasma drift when, as the satellite moves in the dawn-to-dusk direction, either antisunward flow is decreasing or sunward flow is increasing. This associated negative divergence in the dawn-dusk component of the electric field results in a local minimum in the electrostatic potential distribution.

Plate 3 shows a sequence of aurora and global ionospheric convection patterns that are consistent with observations of the aurora, and concurrent IMF measurements, seen in Plate 1. The polar schematics are organised by IMF orientation (in the B_y-B_z plane). The most significant changes in global configuration are shown as B_y changes from negative on the left-hand side (Plates 3a and 3b) to positive on the right-hand side (Plates 3c, 3d, and 3e). Auroral luminosities are illustrated in red; solid black lines denote equipotentials forming simple convection cells, and dotted black lines show another possible closure of the plasma flows indicated by equipotentials.

In Plate 3a an expanded dawnside emission region forms during negative B_y and co-exists with a three-cell convection pattern. The three-cell convection pattern consists of one negative potential cell at lower latitudes on the duskside and two positive potential cells located on the dawnside and is consistent with *Frank et al.* [1986], Figure 10 and *Carlson et al.* [1988], Figure 5. Note that the two positive potential cells on the dawnside may be surrounded by a spatially larger corotating cell. Thus positive potential dominates the electrostatic potential distribution. Note also that a spatially small negative potential cell is shown located

on the dayside to explain the later appearance of four cells [*Cumnock et al.*, 1992]. The poleward edge of the dawnside emission region lies between the two positive potential cells and thus is associated with a local minimum in the positive potential (i.e., near a convection reversal boundary between antisunward flow and sunward flow as the satellite moves along the dawn-to-dusk direction). A possible configuration for the positive B_y case is illustrated by *Nielsen et al.* [1990], Figure 5.

As the IMF becomes more strongly northward (Plate 3b), the positive potential cells become less dominant. The negative potential cell, which originated on the dayside, has moved to higher latitudes between the two positive potential cells and has bifurcated and distorted the large corotating cell. The result is that the poleward edge of the dawnside emission region has moved to higher latitudes. See also *Frank et al.* [1986], Figure 12. Placement of the poleward edge of the dawnside emission region in Plates 3a and 3b is in agreement with the predictions of *Reiff et al.* [1978], and an application of the model to Viking observations [*Jankowska et al.*, 1990].

For B_y slightly positive (Plate 3c), four isolated convection cells are shown, with the high-latitude negative potential cell spatially larger than the high-latitude positive potential cell. Clearing occurs in the dawnside emission region and is associated with increasing antisunward flow (positive electrostatic potential). The transpolar arc is shown centered in the high-latitude negative potential cell and is associated with a convection reversal boundary corresponding to an absolute minimum in the potential distribution.

As B_y becomes increasingly positive (Plate 3d), the negative potential cells may now be surrounded by a spatially larger corotating cell (dotted line) and the high-latitude positive potential cell has moved toward the duskside and become smaller. The high-latitude negative potential cell has moved to higher latitudes with the result that the transpolar arc is now located along the noon-midnight meridian. Thus a theta aurora has been fully formed.

With a further increase in B_y so that it is now greater than B_z (Plate 3e), the negative potential cells have become more dominant. Both the high-latitude negative potential cell and the transpolar arc have moved duskward. As the low-latitude negative potential cell grows and the dayside positive potential cell shrinks further, the duskside auroral oval expands poleward. The dawnside cleared region is now spatially larger than the duskside cleared region. A small cleared region appears where the transpolar arc joins the auroral oval on the nightside. As B_y further increases with respect to B_z one might expect the transpolar arc to continue its duskward movement and the duskside emission region to expand poleward. This may continue until there is no longer a cleared region located on the duskside of the polar region. Thus the configuration can relax to the state described for continually large positive B_y. Alternatively, the transpolar arc may fade as the magnitude of B_y continues to be much larger than B_z, or as the IMF turns southward. We do not illustrate the positive B_y to negative B_y evolution (Plate 2), however we point out that this would not be a mirror image of the negative B_y to positive B_y evolution. In both cases the transpolar arc must be associated with a local minimum in the electrostatic potential distribution (i.e., upward field aligned currents).

4. Summary and Discussion

We have examined five cases where an expanded auroral emission region has evolved into a theta aurora. Our observations show that the evolution of an expanded auroral emission region into a theta aurora requires a large $B_z/|B_y|$ ratio corresponding to a change in the sign of B_y (during northward IMF). Once formed, the theta aurora can persist during various northward and even weakly southward IMF conditions. *Valladares et al.* [1994] also observed a delay in the fading of sun-aligned arcs when the IMF turns southward. In addition, four of our five examples occur when the solar wind velocity is greater than average (> 400 km/s). This observation is consistent with the *Gussenhoven* [1982] finding of an increased occurrence of polar cap arcs with increased solar wind velocity.

Our observations suggest one major difference in the evolution of the auroral patterns depending on the initial sign of B_y. When B_y changes from negative to positive, the dawnside emission region expands to the noon-midnight meridian before the transpolar arc is fully formed; whereas when B_y changes from positive to negative, the duskside emission region only expands midway between the duskside of the auroral oval and the noon-midnight meridian before the transpolar arc is fully formed. These differences are consistent with the differing location in upward field-aligned currents on the dawn and dusk sides of the polar region [*Potemra et al.*, 1984]. *Reiff et al.* [1978] expect upward currents at the flow reversal in the center of the negative potential dusk cell and at the equatorward and poleward edges of the positive potential dawn cell, with the strongest currents located on the duskside. This predicts that sun-aligned arcs on the duskside should be the most intense but that arcs on the dawnside should span a wider range of latitudes than those on the duskside, thereby implying that the evolution of a theta aurora from an expanded duskside emission region is not a mirror image of the evolution of an expanded dawnside emission region.

Observations also suggest that arc motion depends not only on B_y but on the spatial location of the arc within the polar region. Previous observations of arc motion indicated dawn to dusk motion in the morning (evening) sector for negative (positive) B_y, and dawn to dusk (dusk to dawn) motion at highest latitudes for positive (negative) B_y. The *Valladares et al.* [1994] study has refined this picture with the finding that dawnward motion can occur in a dusk cell and duskward motion can take place in a dawn cell for the same value of B_y, but with the size of the cells dependent on the sign of B_y. This is consistent with our observations for positive B_y (Plate 1, 1206 and 1242 UT) where the transpolar arc moves from dawn to dusk while a duskside emission

region forms, expanding dawnward. The opposite case occurs for negative B_y (Plate 2, 1359 and 1424 UT).

The requirement of a change in the sign of B_y for an evolution of a theta aurora to occur, the persistence of a theta aurora after its formation, and the dependence of the arc motion on spatial location, suggest that there may be no clear relationship between the theta aurora pattern and the instantaneous configuration of the IMF.

Acknowledgments.

We wish to thank E. W. Hones Jr. for helping select the imager data used in this study and for fruitful discussions regarding the evolution of the auroral features. We thank L. A. Frank for the use of the DE 1 imager data, the NSSDC for providing the ISEE 3 magnetometer data, and R. A. Frahm and A. Losano for their able technical assistance. The work at the Southwest Research Institute was supported by NASA grant NAG5-1553. Work at the University of Texas at Dallas was supported by NASA grant NAGW-4411. Contributions at the University of Alaska were supported by NASA grant NAGW-3441.

The Editor thanks L. A. Frank and R. J. Pellinen for their assistance in evaluating this paper.

References

Birn, J., W. Hones Jr., J. D. Craven, L. A. Frank, R. Elphinstone, and D. P. Stern, Open and closed field line regions in Tsyganenko's field model and their possible associations with horse-collar auroras, *J. Geophys. Res., 96*, 3811-3817, 1991.

Blomberg, L. G., and G. T. Marklund, High-latitude electrodynamics and aurorae during northward IMF, in *Auroral Plasma Dynamics, Geophys. Monogr. Ser.*, vol. 80, edited by R. L. Lysak, pp. 55-68, AGU, Washington, D. C., 1993.

Burch, J. L., and R. A. Heelis, IMF changes and polar-cap electric field and currents, in *Dynamics of the Magnetosphere*, edited by S.-I. Akasofu, pp. 47-62, D. Reidel, Norwell, Mass., 1979.

Burch, J. L., N. A. Saflekos, D. A. Gurnett, J. D. Craven, and L.A. Frank, The quiet-time polar cap: DE 1 observations and conceptual model, *J. Geophys. Res., 97*, 19403-19412, 1992.

Bythrow, P. F., W. J. Burke, T. A. Potemra, L. J. Zanetti, and T. Y. Lui, Ionospheric evidence for irregular reconnection and turbulent plasma flows in the magnetotail during periods of northward interplanetary magnetic field, *J. Geophys. Res., 90*, 5319-5325, 1985.

Carlson, H. C., R. A. Heelis, E. J. Weber, and J. R. Sharber, Coherent mesoscale convection patterns during northward interplanetary magnetic field, *J. Geophys. Res., 93*, 14501-14514, 1988.

Chiu, Y. T., N. U. Crooker, and D. J. Gorney, Model of oval and polar cap arc configurations, *J. Geophys. Res., 90*, 5153-5157, 1985.

Craven, J. D., and L. A. Frank, Diagnosis of auroral dynamics using global auroral imaging with emphasis on large-scale evolution, in *Auroral Physics*, edited by C.-I. Meng, M. J. Rycroft, and L. A. Frank, pp. 273-288, Cambridge Univ. Press, New York, 1991.

Craven, J. D., J. S. Murphree, L. A. Frank, and L. L. Cogger, Simultaneous optical observations of transpolar arcs in the two polar caps, *Geophys. Res. Lett., 18*, 2297-2300, 1991.

Cumnock, J. A., R. A. Heelis, and M. R. Hairston, Response of the ionospheric convection pattern to a rotation of the interplanetary magnetic field on January 14, 1988, *J. Geophys. Res., 97*, 19449-19460, 1992.

Cumnock, J. A., R. A. Heelis, M. R. Hairston, and P. T. Newell, High-latitude ionospheric convection pattern during steady northward interplanetary magnetic field, *J. Geophys. Res., 100*, 14537-14555, 1995.

Eliasson, L., R. Lundin, and J. S. Murphree, Polar cap arcs observed by the Viking satellite, *Geophys. Res. Lett., 14*, 451-454, 1987.

Elphinstone, R. D., D. Hearn, J. S. Murphree, and L. L. Cogger, Mapping using the Tsyganenko long magnetospheric model and its relationship to Viking auroral images, *J. Geophys. Res., 96*, 1467-1480 , 1991.

Frank, L. A., and J. D. Craven, Imaging results from Dynamics Explorer 1, *Rev. Geophys., 26*, 249-283, 1988.

Frank, L. A., J. D. Craven, K. L. Ackerson, M. R. English, R. H. Eather, and R. L. Carovillano, Global auroral imaging instrumentation for the dynamics explorer mission, *Space Sci. Instr., 5*, 369-393, 1981.

Frank, L. A., J. D. Craven, J. L. Burch, and J. D. Winningham, Polar views of the Earth's aurora with Dynamics Explorer, *Geophys. Res. Lett., 9*, 1001-1004, 1982.

Frank, L. A., J. D. Craven, and R. L. Rairden, Images of the Earth's aurora and geocorona from the Dynamics Explorer mission, *Adv. Space Res., 5(4)*, 53-68, 1985.

Frank, L. A., et al., The theta aurora, *J. Geophys. Res., 91*, 3177-3224, 1986.

Gussenhoven, M. S., Extremely high latitude auroras, *J. Geophys. Res., 87*, 2401-2412, 1982.

Heelis, R. A., P. H. Reiff, J. D. Winningham, and W. B. Hanson, Ionospheric convection signatures observed by DE 2 during northward interplanetary magnetic field, *J. Geophys. Res., 91*, 5817-5830, 1986.

Hones, E. W. J., J. D. Craven, L. A. Frank, D. S. Evans, and P. T. Newell, The horse-collar aurora: A frequent pattern of the aurora in quiet times, *Geophys. Res. Lett., 16*, 37-40, 1989.

Huang, C. Y., J. D. Craven, and L. A. Frank, Simultaneous observations of a theta aurora and associated magnetotail plasmas, *J. Geophys. Res., 94*, 10137-10143, 1989.

Jankowska, K., R. D. Elphinstone, J. S. Murphree, L. L. Cogger, and D. Hearn, The configuration of the auroral distribution of interplanetary magnetic field B_z northward, 2. Ionospheric convection consistent with Viking observations, *J. Geophys. Res., 95*, 5805-5816, 1990.

Kamide, Y., and S.-I. Akasofu, The location of the field-aligned currents with respect to discrete auroral arcs, *J. Geophys. Res., 81*, 3999-4003, 1976.

Lassen, K., C. Danielsen, and C.-I. Meng, Quiet-time average auroral configuration, *Planet. Space Sci., 36*, 791-799, 1988.

Lundin, R., L. Eliasson, and J. S. Murphree, The quiet-time aurora and the magnetospheric configuration, in *Auroral Physics*, edited by C.-I. Meng, M. J. Rycroft, and L. A. Frank, pp. 177-193, Cambridge Univ. Press, New York, 1991.

Meng, C.-I., Polar cap arcs and the plasma sheet, *Geophys. Res. Lett., 8*, 273-276, 1981.

Murphree, J. S., C. D. Anger, and L. L. Cogger, The instantaneous relationship between polar cap and oval auroras at times of northward interplanetary magnetic field, *Can. J. Phys., 60*, 349-356, 1982.

Nielsen, E., J. D. Craven, L. A. Frank and R. A. Heelis, Ionospheric flows associated with a transpolar arc, *J. Geophys. Res., 95*, 21169-21178, 1990.

Potemra, T. A., L. J. Zanetti, P. F. Bythrow, A. T. Y. Lui, and T. Iijima, B_y-dependent convection patterns during northward interplanetary magnetic field, *J. Geophys. Res., 89*, 9753-9760, 1984.

Reiff, P. H., and J. L. Burch, IMF B_y-dependent plasma flow and Birkeland currents in the dayside magnetosphere, 2, A global model for northward and southward IMF, *J. Geophys. Res.*, *90*, 1595-1609, 1985.

Reiff, P. H., J. L. Burch, and R. A. Heelis, Dayside auroral arcs and convection, *Geophys. Res. Lett.*, *5*, 391-394, 1978.

Sharber, J. R., E. W. Hones Jr., R. A. Heelis, J. D. Craven, L. A. Frank, N. C. Maynard, J. A. Slavin, and J. Birn, Dynamics Explorer measurements of particles, fields, and plasma drifts over a horse-collar auroral pattern, *J. Geomagn. Geoelectr.*, *44*, 1225-1237, 1992.

Tsyganenko, N. A., Global quantitative models of the geomagnetic field in the cislunar magnetosphere for different disturbance levels, *Planet. Space Sci.*, *35*, 1347-1358, 1987.

Valladares, C. E., H. C. Carlson, and K. Fukui, Interplanetary magnetic field dependency of stable Sun-aligned polar cap arcs, *J. Geophys. Res.*, *99*, 6247-6272, 1994.

Weiss, L. A., E. J. Weber, P. H. Reiff, J. R. Sharber, J. D. Winningham, F. Primdahl, I. S. Mikkelsen, C. Seifring, and E. M. Wescott, Convection and electrodynamic signatures in the vicinity of a sun-aligned arc: Results from the polar acceleration regions and convection study (Polar ARCS), in *Auroral Plasma Dynamics, Geophys. Monogr. Ser.*, vol. 80, edited by R. L. Lysak, pp. 69-80, AGU, Washington, D. C., 1993.

J. D. Craven, Geophysical Institute, University of Alaska Fairbanks, 903 Koyukuk Drive, P.O. Box 757320, Fairbanks, Alaska 99775-7320

J. A. Cumnock, Space Physics Research Laboratory, University of Michigan, 2455 Hayward Room 1214, Ann Arbor, MI 48109-2143. (e-mail: cumnock@zasu.sprl.umich.edu)

M. R. Hairston and R. A. Heelis, William B. Hanson Center for Space Sciences, University of Texas at Dallas, M.S. FO22, P. O. Box 830688, Richardson, TX 75083-0688

J. R. Sharber, Southwest Research Institute, 6220 Culebra Road, P.O. Drawer 28510, San Antonio, TX 78284

(Received November 11, 1996; revised April 18, 1997; accepted April 21, 1997.)